

## CHAPTER ONE HUNDRED EIGHTY EIGHT

### ANALYSIS OF UPRIGHT STRUCTURE FOR WAVE DISSIPATION USING INTEGRAL EQUATION

Kazuhiro Hagiwara

#### ABSTRACT

A theoretical analysis using an integral equation derived for the unknown horizontal velocity component in a pervious wall is proposed for estimating the reflection and transmission coefficients of upright structures for wave dissipation, and various factors related to wave and structural conditions having influences on the wave dissipating characteristics are investigated for a breakwater with pervious vertical walls at both seaward and landward sides.

In two-dimensional experiments, the theoretical results are in good agreement with experimental data with respect to reflection and transmission coefficients, and therefore, the wave dissipating characteristics of upright structures for wave dissipation can be explained by the integral equation method theory.

#### INTRODUCTION

Recently, the decline of water quality in harbors has become a serious problem in Japan. Therefore, upright breakwaters for wave dissipation such as those with pervious vertical walls at both seaward and landward sides have been constructed for the purposes of reducing reflected wave heights in the harbor, and facilitating exchange of water inside and outside of the harbor. With this type of breakwater, sea water in the protected area can be kept relatively clean to allow the water to pass through the breakwater, but calmness inside the harbor is liable to be disturbed. Consequently, the structural dimensions of this type of breakwater which is required to satisfy the contrasting demands for wave dissipation and water passage must be carefully examined.

A number of theoretical studies such as by Sawaragi and Iwata have been conducted regarding the problem of wave transmission through and reflection from upright structures for wave dissipation. However, equations for calculating the reflection and transmission coefficients are not easily derived.

In this paper, a theoretical method for estimating reflection and

---

Research Engineer, The Research Institute of Shimizu Construction Co., Ltd., 4-17, Etchujima 3-Chome, Kotoku, Tokyo 135, Japan

transmission coefficients of an upright structure for wave dissipation based on an integral equation is proposed while examining various factors related to wave and structural conditions having influences on the dissipating characteristics. In addition, experimental data are utilized to substantiate this theory.

THEORY

Suppose a breakwater, as shown in Figure 1, with pervious vertical walls at both seaward and landward sides, the origin of the coordinate system being taken at the still water surface at the center of the reservoir space with the  $x$  axis horizontal and  $z$  axis vertical and pointing upward. The pervious parts of the front wall with thickness  $b_1$  at  $x = -l$  and of the rear wall with thickness  $b_2$  at  $x = l$  are  $-d_2 \leq z \leq -d_1$  and  $-d_4 \leq z \leq -d_3$ , respectively. Also, suppose that the influence of the discontinuity of water stream is within the limits of  $x_{-2} \leq x \leq x_{-1}$  at the front wall and  $x_1 \leq x \leq x_2$  at the rear wall, respectively, and is very small compared with the wave length. The water area is divided into three regions, (I), (II), and (III).

Assuming a small-amplitude wave in an incompressible perfect liquid in two dimensions with the velocity potential in each region  $\phi_s(x, z; t) = \phi_s(x, z)e^{i\sigma t}$  ( $s=1,2,3$ ), where  $\sigma$  is the incident wave of frequency, then, solutions for Laplace's equation which satisfy surface and boundary conditions are expressed as follows:

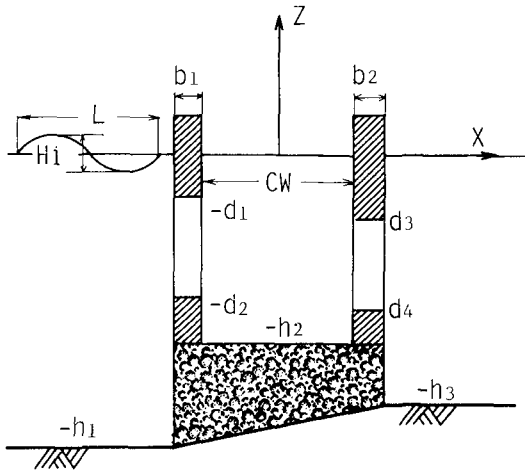


Figure 1 Definition sketch of breakwater with pervious vertical walls at both seaward and landward sides.

$$\begin{aligned} \phi_1(x, z) = & \{A \exp(-ik(x+l+b_1)) + B \exp(ik(x+l+b_1))\} \frac{\cosh k(z+h_1)}{\cosh kh_1} \\ & + \sum_{m=1}^{\infty} C_m \exp(k_m(x+l+b_1)) \frac{\cos k_m(z+h_1)}{\cos k_m h_1} \quad \dots (1) \end{aligned}$$

$$\begin{aligned} \phi_2(x, z) = & (D \frac{\cos k'x}{\cos k'l} + E \frac{\sin k'x}{\sin k'l}) \frac{\cosh k'(z+h_2)}{\cosh k'h_2} \\ & + \sum_{n=1}^{\infty} (F_n \frac{\cosh k_n'x}{\cosh k_n'l} + G_n \frac{\sinh k_n'x}{\sinh k_n'l}) \frac{\cos k_n'(z+h_2)}{\cos k_n'h_2} \quad \dots (2) \end{aligned}$$

$$\begin{aligned} \phi_3(x, z) = & I \exp(-ik''(x-l-b_2)) \frac{\cosh k''(z+h_3)}{\cosh k''h_3} \\ & + \sum_{s=1}^{\infty} J_s \exp(-k_s''(x-l-b_2)) \frac{\cos k_s''(z+h_3)}{\cos k_s''h_3} \quad \dots (3) \end{aligned}$$

where,  $A$  is the known complex constant which represents the incident wave.  $B$  and  $I$  are unknown complex constants representing reflected and transmitted waves, respectively. Also,  $D$ ,  $E$  and  $C_m$ ,  $F_n$ ,  $G_n$ ,  $J_s$  are unknown complex constants for standing and scattered waves, respectively. Further,  $k$ ,  $k_m$ ,  $k'$ ,  $k_n'$  and  $k''$ ,  $k_s''$  are eigenvalues determined by the following relations:

$$\sigma^2 = gk \tanh kh_1 = -gk_m \tan k_m h_1 \quad (m=1, 2, 3, \dots) \quad \dots (4)$$

$$\sigma^2 = gk' \tanh k'h_2 = -gk_n' \tan k_n' h_2 \quad (n=1, 2, 3, \dots) \quad \dots (5)$$

$$\sigma^2 = gk'' \tanh k''h_3 = -gk_s'' \tan k_s'' h_3 \quad (s=1, 2, 3, \dots) \quad \dots (6)$$

where,  $g$  is gravitational acceleration,

Let the horizontal velocity of the pervious part of the vertical wall be  $U_1(z)$  and  $U_2(z)$  at the front and rear walls, respectively. Then the principle of conservation of mass requires the following conditions;

$$U_1(z) = \frac{1}{\epsilon_1} \frac{\partial \phi_1}{\partial x} \Big|_{x_2 \approx -(l+b_1)} = \frac{1}{\epsilon_1} \frac{\partial \phi_2}{\partial x} \Big|_{x_1 \approx -l} \quad \dots (7)$$

$$U_2(z) = \frac{1}{\epsilon_2} \frac{\partial \phi_2}{\partial x} \Big|_{x_1 \approx l} = \frac{1}{\epsilon_2} \frac{\partial \phi_3}{\partial x} \Big|_{x_2 \approx l+b_2} \quad \dots (8)$$

where,  $\epsilon_1$  and  $\epsilon_2$  are opening ratios of the pervious parts of the front and rear walls, respectively. Substituting Eqs. (1), (2) and (3) into Eqs. (7) and (8), we have the following equations:

$$\begin{aligned} \epsilon_1 U_1(z) = & -i(A-B) \frac{k \cosh k(z+h_1)}{\cosh kh_1} + \sum_{m=1}^{\infty} C_m \frac{k_m \cos k_m(z+h_1)}{\cos k_m h_1} \quad \dots (9) \\ = & (D \tan k'l + E \cot k'l) \frac{k' \cosh k'(z+h_2)}{\cosh k'h_2} \end{aligned}$$

$$-\sum_{n=1}^{\infty} (F_n \tanh k_n' l - G_n \coth k_n' l) \frac{k_n' \cos k_n'(z+h_2)}{\cos k_n'h_2} \dots, \dots, (10)$$

$$\begin{aligned} \epsilon_2 U_2(z) = & -(D \tan k' l - E \cot k' l) \frac{k' \cosh k'(z+h_2)}{\cosh k'h_2} \\ & + \sum_{n=1}^{\infty} (F_n \tanh k_n' l + G_n \coth k_n' l) \frac{k_n' \cos k_n'(z+h_2)}{\cos k_n'h_2} \dots, \dots, (11) \end{aligned}$$

$$= -i I \frac{k'' \cosh k''(z+h_3)}{\cosh k''h_3} - \sum_{s=1}^{\infty} J_s \frac{k_s'' \cos k_s''(z+h_3)}{\cos k_s''h_3} \dots, \dots, (12)$$

Considering the orthogonality of the function hyperbolic sine and sine, we multiply each term of Eq. (9) by  $\cosh k(z+h_1)$  and  $\cos k_m(z+h_1)$ , of Eqs. (10) and (11) by  $\cosh k'(z+h_2)$  and  $\cos k_n'(z+h_2)$ , and of Eq. (12) by  $\cosh k''(z+h_3)$  and  $\cos k_s''(z+h_3)$ . In consideration of  $U_1(z) = U_2(z) = 0$  except for  $-d_2 \leq z \leq -d_1$  and  $-d_4 \leq z \leq -d_3$ , integrating from  $z = -h_1$  to  $z = 0$ ,  $z = -h_2$  to  $z = 0$ , and  $z = -h_3$  to  $z = 0$  at each region with respect to  $z$ , we can write the unknown complex constants included in Eqs. (1), (2) and (3).

$$B = A - i \frac{1}{N_0} \int_{-d_2}^{-d_1} \epsilon_1 U_1(\xi) \cosh k(\xi+h_1) d\xi \dots, \dots, (13)$$

$$C_m = \frac{1}{N_m} \int_{-d_2}^{-d_1} \epsilon_1 U_1(\xi) \cos k_m(\xi+h_1) d\xi \dots, \dots, (14)$$

$$\begin{aligned} D = & \frac{1}{2 N_0' \tan k' l} \left[ \int_{-d_2}^{-d_1} \epsilon_1 U_1(\xi) \cosh k'(\xi+h_2) d\xi \right. \\ & \left. - \int_{-d_4}^{-d_3} \epsilon_2 U_2(\xi) \cosh k'(\xi+h_2) d\xi \right] \dots, \dots, (15) \end{aligned}$$

$$\begin{aligned} E = & \frac{1}{2 N_0' \cot k' l} \left[ \int_{-d_2}^{-d_1} \epsilon_1 U_1(\xi) \cosh k'(\xi+h_2) d\xi \right. \\ & \left. + \int_{-d_4}^{-d_3} \epsilon_2 U_2(\xi) \cosh k'(\xi+h_2) d\xi \right] \dots, \dots, (16) \end{aligned}$$

$$\begin{aligned} F_n = & \frac{1}{2 N_n' \tanh k_n' l} \left[ \int_{-d_2}^{-d_1} \epsilon_1 U_1(\xi) \cos k_n'(\xi+h_2) d\xi \right. \\ & \left. + \int_{-d_4}^{-d_3} \epsilon_2 U_2(\xi) \cos k_n'(\xi+h_2) d\xi \right] \dots, \dots, (17) \end{aligned}$$

$$\begin{aligned} G_n = & \frac{1}{2 N_n' \coth k_n' l} \left[ \int_{-d_2}^{-d_1} \epsilon_1 U_1(\xi) \cos k_n'(\xi+h_2) d\xi \right. \\ & \left. + \int_{-d_4}^{-d_3} \epsilon_2 U_2(\xi) \cos k_n'(\xi+h_2) d\xi \right] \dots, \dots, (18) \end{aligned}$$

$$I = i \frac{1}{N_0''} \int_{-d_4}^{-d_3} \epsilon_2 U_2(\xi) \cosh k''(\xi+h_3) d\xi \dots, \dots, (19)$$

$$J_3 = -\frac{1}{N_3''} \int_{-d_4}^{-d_3} \epsilon_2 U_2(\xi) \cos k_S''(\xi+h_3) d\xi \quad \dots\dots(20)$$

where,

$$\left. \begin{aligned} N_0 &= \frac{\sinh 2 kh_1 + 2 kh_1}{4 \cosh kh_1}, & N_m &= \frac{\sin 2 kmh_1 + 2 kmh_1}{4 \cos kmh_1} \\ N_0' &= \frac{\sinh 2 k'h_2 + 2 k'h_2}{4 \cosh k'h_2}, & N_n' &= \frac{\sin 2 k_n'h_2 + 2 k_n'h_2}{4 \cos k_n'h_2} \\ N_0'' &= \frac{\sinh 2 k''h_3 + 2 k''h_3}{4 \cosh k''h_3}, & N_s'' &= \frac{\sin 2 k_S''h_3 + 2 k_S''h_3}{4 \cos k_S''h_3} \end{aligned} \right\} \dots\dots(21)$$

The principle of conservation of momentum at the pervious part of the front wall requires the following condition as shown by Mei et al.:

$$P_{x-2} = P_{x-1} + \rho \left( \frac{1}{2} C_1^* |U_1 e^{i\sigma t}| U_1 e^{i\sigma t} + L_1^* \frac{\partial}{\partial t} (U_1 e^{i\sigma t}) \right) \quad \dots\dots(22)$$

where,  $P$  is fluid pressure,  $\rho$  is fluid density,  $C^*$  is head loss coefficient, and  $L^*$  is apparent orifice length. From the condition in which the energy loss for one period in a linear system is equivalent to that in a non-linear system, the linear resistance coefficient  $f$  is given as follows:

$$f_1^* = \frac{4}{3\pi} C_1^* \bar{U}_1 \quad \dots\dots(23)$$

where,  $u_1 = \bar{U}_1 \sin \sigma t$ . Consequently, Eq. (22) is expressed by the velocity potential as follows:

$$\phi_2|_{x-1} - \phi_1|_{x-2} + \beta_1 \left. \frac{\partial \phi_2}{\partial x} \right|_{x-1} = 0 \quad \dots\dots(24)$$

$$\beta_1 = \frac{1}{\epsilon_1} \left( i \frac{f_1^*}{\sigma} - L_1^* \right) \quad \dots\dots(25)$$

In the same way, we obtain the relationships below with respect to the rear wall,

$$\phi_3|x_2 - \phi_2|x_1 + \beta_2 \left. \frac{\partial \phi_2}{\partial x} \right|_{x_1} = 0 \quad \dots\dots(26)$$

$$\left. \begin{aligned} \beta_2 &= \frac{1}{\epsilon_2} \left( i \frac{f_2^*}{\sigma} - L_2^* \right) \\ f_2^* &= \frac{4}{3\pi} C_2^* \bar{U}_2 \end{aligned} \right\} \dots\dots(27)$$

Substituting Eqs. (1) to (3) into Eqs. (24) and (26), we have the following relationships:

$$\{D(1 + \beta_1 k^t \tan k'l) - E(1 - \beta_1 k^t \cot k'l)\} \cdot \frac{\cosh k'(z+h_2)}{\cosh k'h_2}$$

$$\begin{aligned}
 & + \sum_{n=1}^{\infty} \{F_n(1 - \beta_1 k_n' \tanh k_n' l) - G_n(1 - \beta_1 k_n' \coth k_n' l)\} \\
 & \frac{\cos k_n'(z+h_2)}{\cos k_n'h_2} - (A+B) \frac{\cosh k(z+h_1)}{\cosh kh_1} - \sum_{m=1}^{\infty} C_m \frac{\cos k_m(z+h_1)}{\cos k_m h_1} = 0 \\
 & \dots\dots(28)
 \end{aligned}$$

$$\begin{aligned}
 & \{D(1 + \beta_2 k' \tan k'l) + E(1 - \beta_2 k' \cot k'l)\} \cdot \frac{\cosh k'(z+h_2)}{\cosh k'h_2} \\
 & + \sum_{n=1}^{\infty} \{F_n(1 - \beta_2 k_n' \tanh k_n' l) + G_n(1 - \beta_2 k_n' \coth k_n' l)\} \\
 & \frac{\cos k_n'(z+h_2)}{\cos k_n'h_2} - \frac{\cosh k''(z+h_3)}{\cosh k''h_3} - \sum_{s=1}^{\infty} J_s \frac{\cos k_s''(z+h_3)}{\cos k_s''h_3} = 0 \\
 & \dots\dots(29)
 \end{aligned}$$

Then, substituting Eqs. (13) to (20) into Eqs. (28) and (29) and making a rearrangement, we get, finally, the following results:

$$\epsilon_1 \int_{-d_2}^{-d_1} S_1(z, \xi) U_1(\xi) d\xi + \epsilon_2 \int_{-d_4}^{-d_3} S_2(z, \xi) U_2(\xi) d\xi = A\zeta(z) \dots\dots(30)$$

$$\epsilon_1 \int_{-d_2}^{-d_1} T_1(z, \xi) U_1(\xi) d\xi + \epsilon_2 \int_{-d_4}^{-d_3} T_2(z, \xi) U_2(\xi) d\xi = 0 \dots\dots(31)$$

where,

$$\zeta(z) = \frac{2 \cosh k(z+h_1)}{\cosh kh_1} \dots\dots(32)$$

$$\begin{aligned}
 S_1(z, \xi) &= \frac{\beta_1 k' + \cot 2k'l}{N_0' \cosh k'h_2} \cosh k'(z+h_2) \cosh k'(\xi+h_2) \\
 &+ i \frac{1}{N_0' \cosh kh_1} \cosh k(z+h_1) \cosh k(\xi+h_1) \\
 &+ \sum_{n=1}^{\infty} \frac{\beta_1 k_n' - \coth 2k_n'l}{N_n' \cos k_n'h_2} \cos k_n'(z+h_2) \cos k_n'(\xi+h_2) \\
 &- \sum_{m=1}^{\infty} \frac{1}{N_m \cos k_m h_1} \cos k_m(z+h_1) \cos k_m(\xi+h_1) \dots\dots(33)
 \end{aligned}$$

$$\begin{aligned}
 S_2(z, \xi) &= - \frac{1}{N_0' \sin 2k'l} \frac{1}{\cosh k'h_2} \cosh k'(z+h_2) \cosh k'(\xi+h_2) \\
 &+ \sum_{n=1}^{\infty} \frac{1}{N_n' \sin 2k_n'l} \frac{1}{\cosh k_n'h_2} \cos k_n'(z+h_2) \cos k_n'(\xi+h_2) \dots\dots(34)
 \end{aligned}$$

$$T_1(z, \xi) = S_2(z, \xi) \dots\dots(35)$$

$$\begin{aligned}
 T_2(z, \xi) &= \frac{\beta_2 k' + \cot 2k'l}{N_0'' \cosh k'h_2} \cosh k'(z+h_2) \cosh k'(\xi+h_2) \\
 &+ i \frac{1}{N_0'' \cosh k''h_3} \cosh k''(z+h_3) \cosh k''(\xi+h_3)
 \end{aligned}$$

$$\begin{aligned}
 & + \sum_{n=1}^{\infty} \frac{\beta_2 k_n' - \coth 2k_n' l}{N_n' \cos k_n' h_2} \cos k_n'(z+h_2) \cos k_n'(\xi+h_2) \\
 & - \sum_{s=1}^{\infty} \frac{1}{N_s'' \cos k_s'' h_3} \cos k_s''(z+h_3) \cos k_s''(\xi+h_3) \dots\dots(36)
 \end{aligned}$$

Eqs. (30) and (31) are Fredholm's simultaneous integral equations of the first kind. The integral kernels  $S_1(z, \xi)$ ,  $S_2(z, \xi)$ ,  $T_1(z, \xi)$  and  $T_2(z, \xi)$  are known, while  $U_1(\xi)$  and  $U_2(\xi)$  are unknown functions. These functions cannot be determined analytically except for special problems, and so, they must be solved numerically in terms of approximate values. Then, using weight coefficient  $R_i^n$ , we discretize the integrals of Eqs. (30) and (31) as follows:

$$\left. \begin{aligned}
 \int_{-d_2}^{-d_1} S_1(z, \xi) U_1(\xi) d\xi &= \sum_{i=1}^n R_i^n S_1(z, \xi_i) U_1(\xi_i) (d_2 - d_1) \\
 \int_{-d_4}^{-d_3} S_2(z_1, \xi) U_2(\xi) d\xi &= \sum_{i=1}^n R_i^n S_2(z, \xi_i) U_2(\xi_i) (d_4 - d_3) \\
 \int_{-d_2}^{-d_1} T_1(z, \xi) U_1(\xi) d\xi &= \sum_{i=1}^n R_i^n T_1(z, \xi_i) U_1(\xi_i) (d_2 - d_1) \\
 \int_{-d_4}^{-d_3} T_2(z, \xi) U_2(\xi) d\xi &= \sum_{i=1}^n R_i^n T_2(z, \xi_i) U_2(\xi_i) (d_4 - d_3)
 \end{aligned} \right\} \dots\dots(37)$$

Now, with

$$\begin{aligned}
 f_j &= Af(z_j), \quad U_i^{(1)} = \epsilon_1 (d_2 - d_1) U_1(\xi_i) \\
 U_i^{(2)} &= \epsilon_2 (d_4 - d_3) U_2(\xi_i) \dots\dots(38) \\
 S_{ji}^{(1)} &= S_1(z_j, \xi_i), \quad S_{ji}^{(2)} = S_2(z_j, \xi_i) \\
 T_{ji}^{(1)} &= T_1(z_j, \xi_i), \quad T_{ji}^{(2)} = T_2(z_j, \xi_i)
 \end{aligned}$$

Eqs. (30) and (31) to be finally solved will be the following in terms of matrix expression:

$$\begin{bmatrix} R_1^n S_{11}^{(1)} & \dots & R_n^n S_{1n}^{(1)} & R_1^n S_{11}^{(2)} & \dots & R_n^n S_{1n}^{(2)} \\ \vdots & & \vdots & \vdots & & \vdots \\ R_1^n S_{n1}^{(1)} & \dots & R_n^n S_{nn}^{(1)} & R_1^n S_{n1}^{(2)} & \dots & R_n^n S_{nn}^{(2)} \\ R_1^n T_{11}^{(1)} & \dots & R_n^n T_{1n}^{(1)} & R_1^n T_{11}^{(2)} & \dots & R_n^n T_{1n}^{(2)} \\ \vdots & & \vdots & \vdots & & \vdots \\ R_1^n T_{n1}^{(1)} & \dots & R_n^n T_{nn}^{(1)} & R_1^n T_{n1}^{(2)} & \dots & R_n^n T_{nn}^{(2)} \end{bmatrix} \begin{bmatrix} U_1^{(1)} \\ \vdots \\ U_n^{(1)} \\ U_1^{(2)} \\ \vdots \\ U_n^{(2)} \end{bmatrix} = \begin{bmatrix} f_1 \\ \vdots \\ f_n \\ 0 \\ \vdots \\ 0 \end{bmatrix} \dots\dots(39)$$

For incident wave of  $\eta = (H_T/2) \cdot \cos(k_x - \sigma t)$ , we have constant A in region (I) as follows:

$$A = i \frac{H_I}{2} \frac{g}{\sigma} \exp(ik(l+b_1)) \quad \dots, (40)$$

The values of  $U_i(1)$  and  $U_i(2)$  were determined in this study using the Gauss-Moor method as shown by Hidaka. On obtaining the values, reflection coefficient  $K_R$  and transmission coefficient  $K_T$  can be calculated by Eqs. (13) and (19), respectively.

#### LABORATORY EXPERIMENTS

##### 1. Experimentation Equipment and Procedures

Tests were performed in a two-dimensional wave channel made of steel, 20.0 m long, 0.6 m wide, and 1.0 m deep. The breakwater model having two slotted walls of 2.6-cm thickness was made of vinyl chloride and the front wall was fixed at 14.0 m from the wave generator plate.

The depth of water was maintained constant at 50 cm in the experiments. For wave period of 1.2 sec and incident wave height of 2 cm, the opening ratios  $\epsilon_1$  and  $\epsilon_2$  of the front and rear walls, and the chamber width  $C_w (= 2L)$  were suitably varied.

Capacitance-type wave gages were used to measure wave height. Partial clapotis was measured on the front of the model using a mobile carriage equipped with the wave gages, the reflection coefficient being calculated by Healy's method. The transmitted wave height at a location one-fourth of a wave length back of the model was determined by average of five consecutive wave heights.

##### 2. $C^*$ and $L^*$ of Slotted Wall

The head loss coefficient  $C^*$  and the apparent orifice length  $L^*$  must be determined to calculate the reflection and transmission coefficients. For one slotted wall, Mei et al. gave  $C^*$  as a function of the discharge coefficient and the opening ratio of the wall, and indicated  $L^*$  by the geometric dimensions of the wall on the basis of acoustics. Kondo and Sato connected  $C^*$  and  $L^*$  of one perforated wall with drag coefficient  $C_D$  and inertia coefficient  $C_M$  of the wall, respectively, and gave  $C^*$  as a function of both opening ratio and Reynolds number. Also, they gave the non-dimensional parameter  $L^*/L$  ( $L$ : incident wave length) as a function of the Keulegan-Carpenter number. For a caisson with a slotted front wall, Tanimoto and Yoshimoto gave  $C^*$  as a function of the opening ratio of the wall, and also, the non-dimensional parameter of  $L^*$  and the wall thickness as a function of the ratio of chamber width to wave length of the chamber. They obtained an experimental formula of  $C^*$  and  $L^*$  by minimizing the square sum of the difference between the calculated and experimental values related to the reflection coefficient. In this paper,  $C^*$  and  $L^*$  are related to  $C_D$ ,  $C_M$  and the geometric dimensions of the slotted wall, respectively, on the basis of an approach similar to that of Kondo and Sato.

To consider the equilibrium of force on the pervious wall in unsteady flow, it can be expressed as "forces generating flow" = "inertia force of fluid" + "force acting on body." The force acting on the body

can then be expressed separating into drag force and inertia force as follows:

$$Fd = \rho V_f \frac{dq}{dt} + (\rho C_D A_S \frac{|q| \cdot q}{2} + \rho C_M V_S \frac{dq}{dt}) \quad \dots (41)$$

where,  $q$ : fluid velocity in the opening part of the pervious wall,  $V_f$ : volume of fluid,  $V_S$ : volume of the non-opening part of the pervious wall,  $A_S$ : projected area of the non-opening part of the pervious wall.

As the forces which generate flow are due to the pressure gradient between the front and back of the pervious wall, Eq. (41) may be rewritten as follows:

$$-\frac{1}{\rho} \frac{\partial P}{\partial x} = C_D \left( \frac{A_S}{V_T} \right) \frac{|q|q}{2} + \left( \frac{V_f}{V_T} + C_M \frac{V_S}{V_T} \right) \frac{dq}{dt} \quad \dots (42)$$

Using the opening ratio  $\epsilon$  and the wall thickness  $\Delta x$ , Eq. (42) may be expressed as:

$$-\frac{1}{\rho} \frac{\partial P}{\partial x} = C_D \frac{1-\epsilon}{\Delta x} \frac{|q|q}{2} + \{ \epsilon + C_M(1-\epsilon) \} \frac{dq}{dt} \quad \dots (43)$$

Meanwhile, the equation of motion of flow in the vicinity of the pervious wall is expressed by Eq. (22) which can be rewritten as follows:

$$-\frac{1}{\rho} \frac{P}{x} = C^* \frac{1}{\Delta x} \frac{|q|q}{2} + L^* \frac{1}{\Delta x} \frac{\partial q}{\partial t} \quad \dots (44)$$

As Eqs. (43) and (44) are equivalent,  $C^*$  and  $L^*$  will be the following:

$$\left. \begin{aligned} C^* &= C_D(1-\epsilon) \\ L^* &= \epsilon \{ 1 + C_M(1-\epsilon) \} \Delta x \end{aligned} \right\} \quad \dots (45)$$

For the inertia coefficient, we use  $C_M = 2.19$  obtained from the potential theory for a square pillar. For the drag coefficient, the following is considered. From Hino and Yamasaki, the quantity of energy dissipation per period is expressed as shown below.

$$\delta = \int_0^T F(t)q(t)dt \quad \dots (46)$$

where, the force  $F(t)$  on the pervious wall and the velocity  $q(t)$  at the opening part of the pervious wall are hypothesized as follows:

$$\left. \begin{aligned} F(t) &= \frac{1}{2} C_D \rho (1-\epsilon) h |q(t)|q(t) \\ q(t) &= q_0 \sin \sigma t \end{aligned} \right\} \quad \dots (47)$$

Substituting Eq. (47) into Eq. (46), we have the following relationship:

$$\delta = \frac{2TC_D \cdot \rho(1-\epsilon)h q_0^3}{3\pi} \dots\dots(48)$$

With  $q_0$  as the average value of the  $Z$  direction at the time phase when  $q(t)$  in Eq. (47) is at the maximum,  $q_0$  is expressed as follows:

$$q_0 = \frac{1}{h} \int_{-h}^0 \frac{1}{\epsilon} \frac{\pi H I}{T} \frac{\cosh k(z+h)}{\sinh kh} dz \dots\dots(49)$$

Consequently, substituting Eq. (49) into Eq. (48),  $\delta$  will be as follows:

$$\delta = \frac{2\pi^2 H I^3 (1-\epsilon) \rho C_D h}{3T^2 \epsilon^3 (kh)^3} \dots\dots(50)$$

or

$$\frac{\delta}{W} = C_D \frac{1-\epsilon}{\epsilon^3} \frac{1}{(kh)^3} \dots\dots(51)$$

where,

$$W = \frac{2\pi^2 H I^3 h}{3g T^2} \dots\dots(52)$$

In this case,  $\delta/W$  indicates the non-dimensional quantity concerning energy dissipation at the pervious wall. We examine  $C_D$  by means of comparing the calculated results with the experimental ones.

The ratio of energy dissipation  $E_I$  for the incident wave is expressed by the reflection coefficient  $K_R$  and the transmission coefficient  $K_T$  as follows:

$$E_I = 1 - K_R^2 - K_T^2 \dots\dots(53)$$

Hence, the quantity of energy dissipation is obtained by multiplying  $E_I$  by the energy and period of the incident wave:

$$\delta = E_t(E \cdot C_g) i \cdot T = (1 - K_R^2 - K_T^2) \cdot \frac{1}{8} \rho g H i^2 \cdot C_g i \cdot T \dots\dots(54)$$

where,  $C_g i$  indicates the group velocity of the incident wave, and is expressed as follows:

$$\left. \begin{aligned} C_g i &= n \cdot C_i \\ n &= \frac{1}{2} \left[ 1 + \frac{2 kh}{\sinh 2 kh} \right] \end{aligned} \right\} \dots\dots(55)$$

where,  $C_i$  is wave velocity. Dividing Eq. (54) by  $W$ , the non-dimensional expression with  $C_D$  corresponding to Eq. (51) as the parameter is obtained.

Figure 2 presents comparisons of  $\delta/W$  between the calculated results by Eq. (51) and the measured ones for the single-slotted wall. These results indicate that the measured values can be approximated by the calculated curve for  $C_D = 2.05$ . Also, Urashima et al. found  $C_D =$

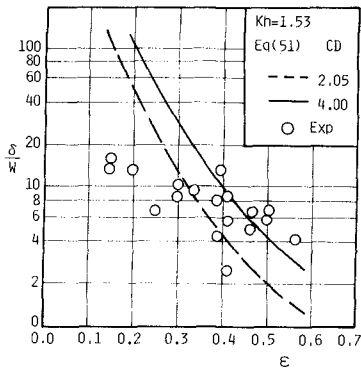


Figure 2 Experimental and theoretical  $\delta/W$ .

2.05 and  $C_M = 2.19$  could be approached when flow velocity was defined by the actual velocity in the slot, and consequently, in this paper,  $C_D = 2.05$  was adopted for both the front and rear walls.

3. Comparisons Between Experiment and Theory

Figure 3 shows comparisons of the reflection and transmission coefficients between experiments and theory for a breakwater having a single vertical slotted wall. The measured values are in good agreement with the theory.

Figures 4 and 5 show comparisons of the experimental and theoretical reflection and transmission coefficients for a breakwater having vertical slotted walls at both the seaward and landward sides. These figures indicate a tendency for theoretical values to be in agreement with measured values, though the latter are generally smaller than the calculated results in Figure 4.

This theory is then compared with the experimental results of other researchers, Figure 6 shows comparisons of the reflection and transmission coefficients from experiments by Kono and Tsukayama and from this theory for a submerged breakwater. As for Figure 7, it shows a comparison of the transmission coefficient from experiments by Kato and Jouman and this theory for double rigid thin barriers. The theoretical results for each type of breakwater are in good agreement with

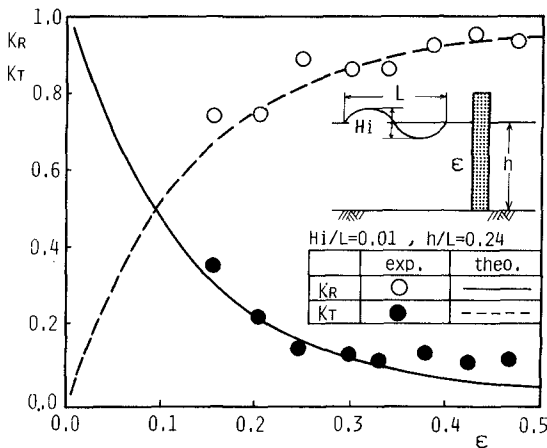


Figure 3 Breakwater with single vertical slotted wall.

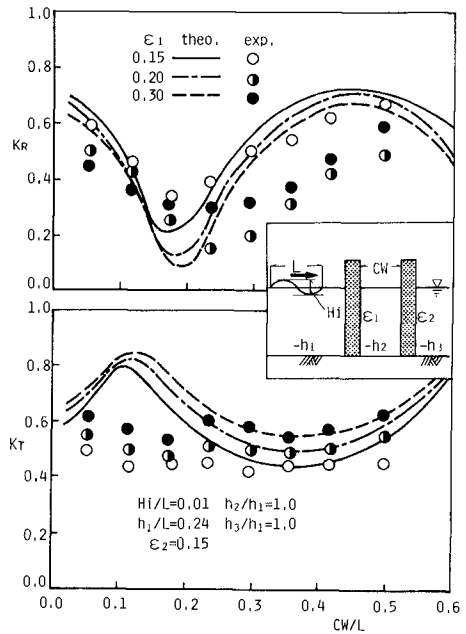


Figure 4 Breakwater with double vertical slotted walls. Plots of  $K_R$ ,  $K_T$  versus  $CW/L$ .

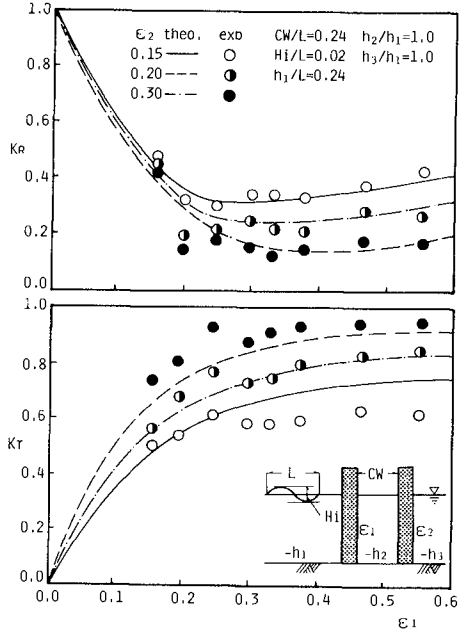


Figure 5 Breakwater with double vertical slotted walls. Plots of  $K_R$ ,  $K_T$  versus  $\epsilon_1$ .

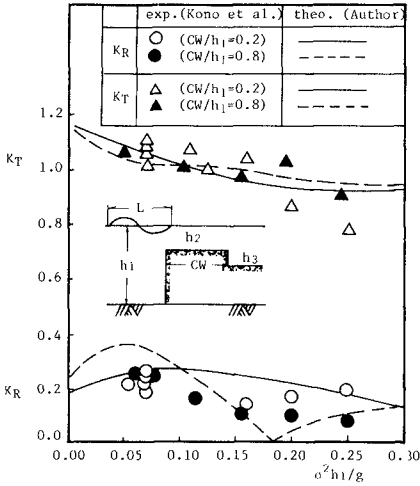


Figure 6 Submerged breakwater.

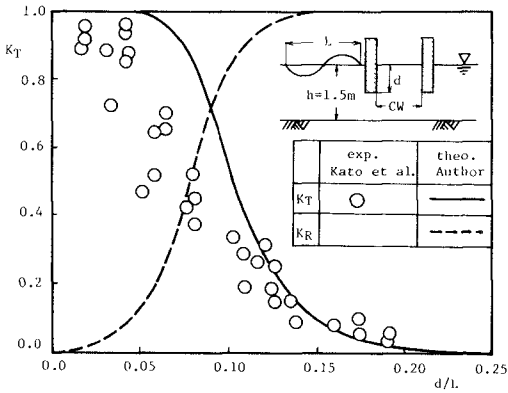


Figure 7 Double rigid thin barriers.

measured results of other researchers. Consequently, it has been found that the wave dissipating characteristics of the upright structures can be explained well by the integral equation method theory.

VARIOUS FACTORS HAVING INFLUENCES ON REFLECTION AND TRANSMISSION COEFFICIENTS

Suppose a prototype breakwater with pervious vertical walls at both seaward and landward sides and examine various factors having influences on the reflection and transmission coefficients, numerically.

Figure 8 shows the relationships between the reflection and

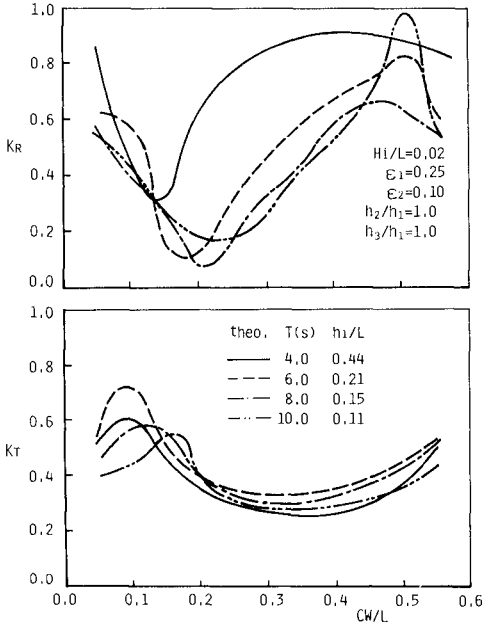


Figure 8  $K_R$ ,  $K_T$  and  $C_W/L$ .

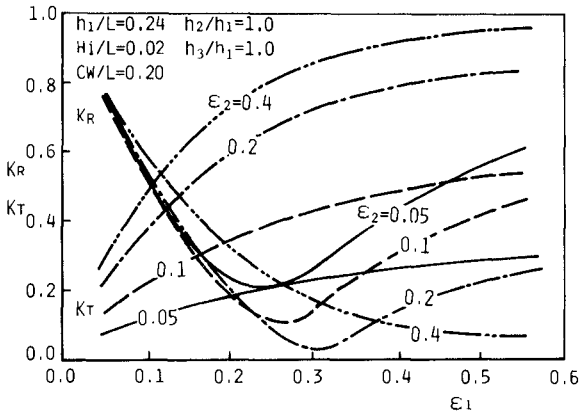


Figure 9  $K_R$ ,  $K_T$  and  $\epsilon$ .

transmission coefficients  $K_R$ ,  $K_T$  and the relative chamber width  $C_W/L$  under the conditions of  $\epsilon_1 = 0.25$ ,  $\epsilon_2 = 0.1$  and  $H_I/L = 0.02$ . The reflection coefficient is a minimum at  $C_{W0}/L$  making the wave energy dissipation maximum. The value of  $C_{W0}/L$  changes by the period  $T$ , that is, the relative water depth  $h_1/L$ , and becomes large for the smaller values of  $h_1/L$ . The transmission coefficient does not change as much as the reflection coefficient for the relative chamber width and the period.

Figure 9 shows the relationships between the reflection and transmission coefficients and the opening ratios for the front and rear pervious walls under the conditions of  $H_I = 1.0$  m,  $T = 6.0$  sec, and  $C_W/L = 0.2$ .

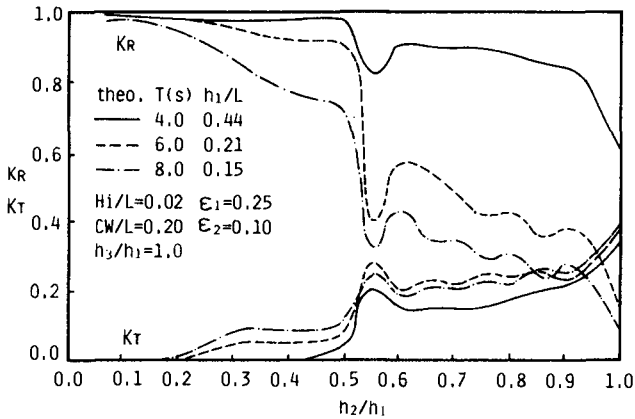


Figure 10  $K_R$ ,  $K_T$  and  $h_2/h_1$ .

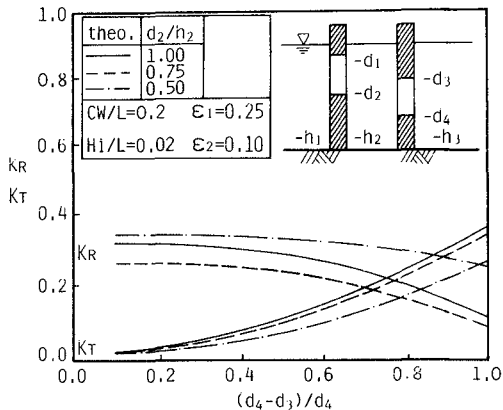


Figure 11  $K_R$ ,  $K_T$  and depth of pervious wall.

The value of  $\epsilon_1$  taking the minimum value of  $K_R$  is small as  $\epsilon_2$  decreases, but the minimum value of  $K_R$  is small as  $\epsilon_2$  increases.  $K_T$  increases as the values of both  $\epsilon_1$  and  $\epsilon_2$  become larger and larger. Consequently, the opening ratios of the front and rear pervious walls having influences on  $K_R$  and  $K_T$  are important, so it is possible to make the values of both  $K_R$  and  $K_T$  small by choosing the opening ratios appropriately.

The relationships between the reflection and transmission coefficients and the water depth in the chamber under the conditions of  $\epsilon_1 = 0.25$ ,  $\epsilon_2 = 0.1$ , and  $C_W/L = 0.25$  are shown in Figure 10. As the values of relative water depth  $h_2/h_1$  become larger and larger,  $K_R$  decreases and  $K_T$  increases, that is, as the water depth in the chamber becomes deeper than one-half of the water depth in front of the breakwater,  $K_R$  decreases suddenly depending on the period, although some amount of waves is let through to the back.

Figure 11 shows the relationships between the reflection and transmission coefficients and depth of the pervious wall under the conditions of  $H_I = 1.0$  m,  $T = 6.0$  sec,  $\epsilon_1 = 0.25$ ,  $\epsilon_2 = 0.1$ , and  $C_W/L = 0.2$ . As the depth of the rear pervious wall becomes greater,  $K_R$  decreases slightly although  $K_T$  increases gradually. Also, the depth of the front pervious wall has a great influence on  $K_R$  more than on  $K_T$ .

#### CONCLUSIONS

- (1) An analytical solution of reflection and transmission coefficients has been derived for an upright breakwater with pervious walls at both seaward and landward sides based upon an integral equation.
- (2) The head loss coefficient and apparent orifice length in the present theory have been related to the drag and inertia coefficients in the wave force equation and the geometric dimensions of the slotted wall, respectively.
- (3) The theoretical results of each type of upright breakwater have been compared with the experimental results of the author and other researchers, and as a result, it has been found that the wave dissipating characteristics of the upright structure with the pervious wall can be explained well by the present theory.
- (4) For the purpose of making both the values of the reflection and transmission coefficients small, it is important to determine the relative chamber width and the opening ratio of the pervious wall appropriately.

#### REFERENCES

- For example, Hidaka, K., "Theory of Applied Integral Equation," Gendai-sha, 1974 (in Japanese).
- Hino, M., and Yamasaki, T., "Reflection and Transmission Coefficient, and Energy Loss of Surface Wave by a Vertical Barrier," Proc. of Japan

Society of Civil Engineers, No. 190, 1971 (in Japanese).

Kato, J., and Jouman, T., "Wave Dissipating Effect of Double Curtain-Wall Breakwater," Proc. of 15th Coastal Engineering Conf. in Japan, 1968 (in Japanese)

Kondo H., and Sato, R., "Presumption of Head Loss and Apparent Orifice Length of Porous Walls," Proc. of 26th Coastal Engineering Conf. in Japan, 1976 (in Japanese).

Kono, T., and Tsukayama, S., "Wave Deformation on a Barrier Reef," Proc. of Japan Society of Civil Engineers, No. 307, 1981 (in Japanese).

Mei, C. C., Liu, P. L. F., and Ippen, A. T., "Quadratic Loss and Scattering of Long Waves," Proc. ASCE, Vol. 100, No. WW3, 1974.

For Example, Sawaragi., T., and Iwata, K., "On Wave Absorber of Two Permeable Walls Type Breakwater Quay," Proc. of Japan Society of Civil Engineers, No. 262, 1977 (in Japanese).

Tanimoto, K., and Yoshimoto, Y., "Various Factors Having Influences on the Reflection Coefficient for Wave Dissipating Caisson with a Slotted Front Wall," Proc. of 29th Coastal Engineering Conf. in Japan, 1982 (in Japanese).

Urashima, S., Ishizuka, K., and Kondo, H., "Characteristics of Wave Force on a Slotted Wall," Tomakomai Technical College, No. 17, 1982 (in Japanese).